
Attack on Multi-Node Attention for Object Detection

Sizhe Chen¹Fan He¹Xiaolin Huang^{1*}Kun Zhang²¹Shanghai Jiao Tong University, Shanghai, 200240, P.R. China²Carnegie Mellon University, Pittsburgh, PA 15213, USA

Abstract

This paper focuses on high-transferable adversarial attacks on detection networks, which are crucial for life-concerning systems such as autonomous driving and security surveillance. Detection networks are hard to attack in a black-box manner, because of their multiple-output property and diversity across architectures. To pursue a high attacking transferability, one needs to find a common property shared by different models. Multi-node attention heat map obtained by our newly proposed method is such a property. Based on it, we design the ATTACK on multi-node attention for object detection (ATTACTION). ATTACTION achieves a state-of-the-art transferability in numerical experiments. On MS COCO, the detection mAP for all 7 tested black-box architectures is halved and the performance of semantic segmentation is greatly influenced. Given the great transferability of ATTACTION, we generate Adversarial Objects in Context (AOCO), the first adversarial dataset on object detection networks, which could help designers to quickly evaluate and improve the robustness of detection networks.

1 Introduction

Adversarial attacks [1, 2, 3, 4, 5, 6] have revealed the fragility of Deep Neural Networks (DNNs) by cheating them with elaborately-crafted but imperceptible perturbation. Among them, black-box attack, i.e., attacking without knowledge of the inner structure and weights, is much harder and more aggressive because it is closer to real-world attacking scenarios. For classification networks, there exist some promising black-box attacks [7, 8, 9, 10, 11, 12], which greatly influence the network performance. Also severe is to attack object detection [13] in a black-box manner, e.g., hide certain objects from detectors [14]. By that, life-concerning systems based on object detection such as autonomous driving and security surveillance would be greatly influence.

To the best of our knowledge, no existing attack is specifically designed for black-box transferability in detection networks. The main reason is that no common property across detection nets has been found, which, however, is essential to high transferability [12]. In this paper, we concentrate on the attention heat maps, on which different detection nets have similar results as shown in Fig. 1. Although some works have adopted the attention heat map as an indicator of a success attack [15, 16, 12], we are the first to directly attack the attention of detection networks, i.e., include it in the attack loss.

We design the ATTACK on multi-node attention for object detection (ATTACTION). ATTACTION focuses on suppressing the attention rather than directly changing the prediction as in existing works [17, 18, 19]. Since the heat maps are quite similar across models, those of other black-box models are influenced as well, leading to the black-box transferability.

However, the attention heat map for detection nets is difficult to obtain. Because their predictions are formed by multiple output i.e., information for several bounding boxes, but existing methods [20, 21, 22] to calculate the attention are all designed for classification nets with the single-node

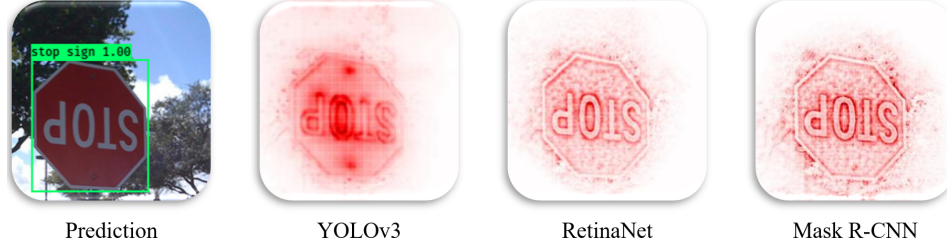


Figure 1: Attention heat maps for models with different architectures by our MN-SGLRP. Three models not only predict the “stop sign” right, but also share a similar attention property.

prediction. Accordingly, they could not be directly adopted in detection nets, so we propose Multi-Node Softmax Gradient Layer-wise Relevance Propagation (MN-SGLRP) for object detection.

Based on the calculated heat map, a common property across architectures, ATTACTION is designed and achieves a state-of-the-art transferability on 7 black-box models for COCO [23] dataset, nearly halving the mAP. ATTACTION is also flexible to be combined with other techniques [9, 15, 11] for better transferability. Interestingly, the adversarial samples of ATTACTION also greatly influence the performance of semantic segmentation, even the attacked model is for detection only.

Given the high transferability of ATTACTION, we create Adversarial Objects in CONtext (AOCO), the first adversarial dataset for object detection. AOCO contains 10000 samples that significantly decrease the performance of black-box models for detection and segmentation. AOCO may serve as a new benchmark to evaluate the robustness of DNNs or improve it by adversarial training.

Contributions

- We design MN-SGLRP, the first method to **visualize and interpret detection nets**.
- Based on MN-SGLRP, we propose a novel attack named ATTACTION, which is the first attack **specifically designed for black-box transferability** in detection nets.
- We evaluate ATTACTION on MS COCO dataset and verify its state-of-the-art **transferability across models and tasks**.
- By ATTACTION, we create AOCO, the **first adversarial dataset for detection** networks.

2 Related Work

Since [1], there have been lots of promising adversarial attacks [2, 3, 4, 5, 6, 12]. Generally, they fix the network weights and change the input x slightly to optimize the attack loss. The network then predicts incorrectly on adversarial samples with a high confidence. [7, 24] find that adversarial samples may transfer to other black-box models as well. Input modification [9, 11, 15] or other optimization ways [10, 11] are able to increase the transferability. These techniques are designed for the attack in classification, but could also be combined with our ATTACTION.

[17] extends adversarial attack to detection networks. It adopts classification loss and proposes to attack on densely generated bounding boxes. After that, losses about localization and classification are designed [18] for attack. [19, 25] propose to attack detectors with perturbation in a restricted area. Existing works achieve good results in white-box scenarios, but are not specifically designed for black-box transferability, which is quite limited (a 5 to 10% decrease from the original mAP) even when two models only differ in backbone [17, 18, 26]. [27] discusses black-box attack based on queries rather than the transferability as we do. The performance is satisfactory, but it requires over 30K queries, which is easy to be found by the model owner.

To calculate common properties across models and increase the attack transferability, we resort to network visualization methods [28, 29, 30]. They are originally developed to interpret how DNNs predict and help users gain trust on them. Specifically, they display how the input contributes to a certain node output in a pixel-wise manner. Typical works include Layer-wise Relevance Propagation (LRP) [20], Contrastive LRP [21] and Softmax Gradient LRP (SGLRP) [22]. However, they could only visualize the attention for a single target node in classification nets.

3 Attack on Multi-Node Attention for Object Detection

We propose an attack specifically designed for black-box transferability, named ATTACK on multi-node attention for object detection (ATTACKTION). ATTACKTION works by suppressing multi-node attention for several bounding boxes. Since the attention heat map is commonly shared by different architectures as shown in Fig. 1, attacking on it in the white-box surrogate model achieves a high transferability towards black-box models. Below we first analyse why we do not adopt the high-transferable single-node attack on attention in classification. Then we present our ATTACKTION framework and introduce its details by addressing three crucial issues.

3.1 Why Attention and Why Not Single-Node Attention

Classification nets [31, 32, 33, 34] generally output a vector y . The decision is formed by the largest probability $\arg \max(y)$, which is single-node information. So, [12] proposes to attack on single-node attention (AoA), i.e., suppresses the attention for the correct class, and achieve a good transferability.

However, it does not work well in attacking detection nets given their large difference compared to classification ones. In contrast to classification nets, predictions of detection nets [35, 36, 37, 38], or the messages presented to the users, are formed by the location and confidence of several bounding boxes, which is multi-node information. [17] discusses the necessity of attacking multi-node output in detection nets and many works also validate that [18, 25, 26].

According to the analysis above, it can be expected that single-node attention attacks in classification are ineffective for attacking detection networks. Experimental validation of this is presented in the Supplement Material.

3.2 Who is ATTACKTION

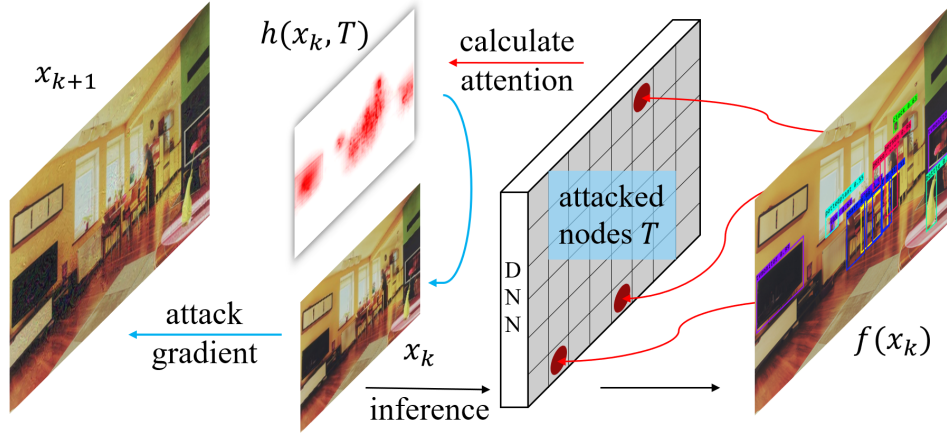


Figure 2: Framework of ATTACKTION. x_k is the sample in iteration k and $f(x_k)$ is the network prediction for it. MN-SGLRP calculates the network attention heat map $h(x_k, T)$ for certain target nodes in set T . Gradients of $h(x_k, T)$ back propagate to x_k , which is then modified to x_{k+1} .

To achieve a high transferability in attacking object detection, we propose to ATTACK on multi-node attention for object detection (ATTACKTION). We present the framework of ATTACKTION in Fig. 2. Starting from the original sample x_0 , the input image x_k in the k -th iteration forward propagates in the surrogate model and gets the prediction $f(x_k)$. Then the network visualization method calculates the attention heat map $h(x_k, T)$ for all attacked nodes in set T . Gradients of $h(x_k, T)$ back propagate through the whole route to x_k , which is then modified to x_{k+1} .

In this framework, there are three crucial issues: (i) how to get the attention heat map $h(x, T)$; (ii) how to update the sample x by gradients of $h(x, T)$; (iii) how to choose the multiple nodes to attack.

3.3 What is the Attention for Detection

Among the visualization methods for classification [20, 21], SGLRP [22] excels in discriminating ability against irrelevant regions of a certain target node. It visualizes how the input contributes to one output node by back-propagating the relevance from the output to the input. R is the initial relevance in the output layer and its n -th component is calculated as

$$R_n = \begin{cases} y_n (1 - y_n) & n = t \\ -y_t y_n & n \neq t, \end{cases} \quad (1)$$

where y_n is the predicted probability of class n , and y_t is that for the single-node target t . The pixel-wise attention heat map $h(x, t)$ for the single-node target t is calculated by back propagating the relevance R from the final layer to the input with rules specified in [22].

In detection nets, we mostly wonder how the input contributes to m bounding boxes. This multi-node attention could not be directly calculated by (1). The intuitive idea of simply adding m single-node heat maps is inefficient and not applicable. Since in this way, the heat map needs to be calculated m times for m single-node targets. Besides, the added heat map is different from the multi-node attention. Because in SGLRP, the “irrelevant” regions for one target node (all $n \neq t$ in (1)) are suppressed, which may be the relevant regions for other target nodes. Adding all single-node heat maps together actually suppresses all relevant regions for $m - 1$ times but only highlights it for 1 time, which is not our intention to calculate the multi-node attention.

Here we present our Multi-Node Softmax Gradient Layer-wise Relevance Propagation (MN-SGLRP), the first network visualization method for detection networks and therefore contribute to the high-transferable attack, which is modified from SGLRP as

$$R_n = \begin{cases} y_n (1 - y_n) & n \in T \\ -\frac{1}{m} \sum_{i=1}^m y_{t_i} y_n & n \notin T, \end{cases} \quad (2)$$

where y_{t_i} is the predicted probabilities for one target node t_i . T is the set containing all target nodes $\{t_1, t_2, \dots, t_m\}$. In this way, relevance for all target nodes is calculated in one time as we desire. Therefore, the heat map is obtained very quickly, i.e., m times faster than adding single-node ones.

We illustrate the difference between single-node SGLRP and our multi-node MN-SGLRP in Fig. 3. SGLRP only displays the network attention for one node of one bounding box, e.g. TV, chair, bottle, as shown in the right 3 images. MN-SGLRP, in contrast, visualizes the overall attention for several nodes. It could also demonstrate the relative attention strength for different nodes, e.g., the attention for bottle is smaller than that for TV as shown in the second image.



Figure 3: Difference between heat maps from SGLRP and MN-SGLRP. The heat maps are for YOLOv3 [37]. For SGLRP, we choose the object confidence nodes for the predicted bounding boxes “TV”, “chair” and “bottle” for demonstration. For MN-SGLRP, 20 object confidence nodes with the highest values are chosen.

3.4 How to Update the Sample

For the update, we choose the simple one in our baseline as

$$x_{k+1} = \text{clip}_\varepsilon \left(x_k - \alpha \frac{g(x_k)}{\|g(x_k)\|_1/N} \right), \quad (3)$$

$$g(x) = \frac{\partial h(x, T)}{\partial x},$$

where α stands for the step length. x is l_∞ -norm bounded by ε from the original sample in each iteration. Gradient $g(x)$ is normalized by its average l_1 -norm, i.e., $\|g(x)\|_1/N$ to prevent numerical

errors and control the degree of perturbation. N is the dimension of the image. In Section 4, we will show that the transferability of ATTACTION is further increased from the baseline by adopting other update formulas [9, 11, 15].

3.5 Where to Attack

It is important to choose a proper node set T to attack. Choices of localization or classification nodes are described in [13]. Attack that adopts the localization loss moves or shrinks the bounding boxes. Attacking by the classification loss, in contrast, leads the bounding boxes to be in a different class or even disappear.

Although these two losses are coupled by the shared layers and the Non-Maximum Suppression in the output [13]. We observe that they differ in the performance as losses for attack. The results are presented in Table 1, where Dfool [25] uses the classification loss and Loc adopts the localization loss. Generally, localization loss leads to a greater drop in white-box cases, but the classification loss induces better black-box transferability. Accordingly, we choose to attack m classification nodes T with the highest confidence.

Intuitively, a large m leads to attack on more bounding boxes, which, meanwhile, leads to a large GPU memory occupation. A smaller m may cause a focus on fewer bounding boxes. In the extreme case when $m = 1$, the multi-node ATTACTION is reduced to single-node AoA. To trade off, we suggest $m = 20$ in ATTACTION empirically.

4 Experiments

In this section, we evaluate the performance of ATTACTION, especially its transferability. The results are presented numerically and visually. In comprehensive evaluation, ATTACTION achieves a great transferability in across models and even across tasks. Furthermore, ATTACTION is flexible be easily combined with existing transfer-enhancing techniques for a better performance.

4.1 Setup

Our experiments are conducted on Keras [39], Tensorflow [40] and PyTorch [41] in 4 NVIDIA GeForce RTX 2080Ti GPUs. Library iNNvestigate [42] is used to implement MN-SGLRP.

We experiment on MS COCO 2017 dataset [23], which is a large-scale benchmark for object detection, instance segmentation and captioning. It contains over 118K training images and 5K validation samples. For a fair evaluation, we generate adversarial samples from all 5K samples in its validation set each time and test several black-box models on their mAP, a standard criteria in many works [35, 36, 38]. mAP is calculated by APIs provided in [23]. All attacks are conducted with the step size $\alpha = 2$ for 10 iterations and the perturbation is l_∞ -bounded in $\varepsilon = 16$ to guarantee the imperceptibility as in [15, 11].

The black-box well-trained models from MMDetection [43] are M1 (SSD512 [44]), M4 (Faster R-CNN [35]), M6 (Cascade R-CNN [45]), M7 (Cascade Mask R-CNN [45]), M8 (Hybrid Task Cascade [38]). We choose the best backbones for all models we use in MMDetection and specify them in the Supplementary Material. The surrogate models we attack include M2 [46] (YOLOv3 [37]), M3 [47] (RetinaNet [48]) and M5 [49] (Mask R-CNN [36]) as representations for single-task models and multi-task ones. To pre-process, we resize the image with its long side as 416 for YOLOv3 or RetinaNet and 448 for Mask R-CNN, and then zero-pad it to a square. The resolution is kept relatively the same for a fair evaluation. Images are normalized to $[0,1]$ in YOLOv3 or subtracted by the mean of COCO training set in RetinaNet and Mask R-CNN.

To validate that the aggression comes from the attack method rather than resizing or random perturbation, we add the Gaussian noise ($\sigma = 9$) to images resized to 416 and make the perturbation larger than any other experiments. This ablation results are reported as ‘‘Ablation’’. The original mAP for MS COCO validation set provided in MMDetection is reported as ‘‘None’’ (attack).

4.2 Transferability of ATTACTION

We first evaluate the transferability of ATTACTION baseline with other detection attacks in the same setting. For DAG [17], we follow the setting of generating dense proposals. The classification probabilities of 3000 bounding boxes with highest confidence are attacked. But we alter its optimization to (3) because its original update produces quite small perturbation, leading to a poor transferability, which is unfair for comparison. Dfool [25] suppresses the classification confidence for the original bounding boxes, which is the same in our experiment. Localization loss is shown to be useful in [13], and here we suppress the width and height of the original bounding boxes. In ATTACTION, there are rare cases (less than 5% iterations) when the attention is too small to calculate the gradient. In these cases, we resort to DAG loss, and the gradient would recover in one iteration.

We present the mAP of several victim networks in adversarial samples crafted by attacking M2 (YOLOv3 [37]) with different methods in Table 1. It could be seen that ATTACTION enjoys a state-of-the-art transferability towards 7 black-box models, outperforming other methods for about 10% (2 to 3 mAP). ATTACTION also maintains a good performance in white-box attack, but is not the best since it is specifically designed for black-box scenarios. The mAP50 and mAP75 follow the same trend and are reported in the Supplement Material. In ablation experiment in the second row, we find that the aggression of adversarial samples comes from method rather than the perturbation.

Table 1: mAP of object detection in different attacks on M2 (YOLOv3)

Method	M1	M2	M3	M4	M5	M6	M7	M8
None	29.3	33.4	38.1	40.7	42.1	42.5	45.7	46.9
Ablation	24.9	31.4	31.2	31.6	35.0	34.3	37.5	38.8
Dfool	23.3	2.5	29.2	29.8	33.3	32.9	36.5	38.0
Loc	21.9	0.2	25.8	26.6	29.8	29.4	33.2	33.2
DAG	20.8	0.6	22.8	23.4	26.8	25.6	28.9	31.0
ATTACTION	18.1	1.2	19.9	20.5	24.3	22.6	26.4	28.2

4.3 Transferability with Transfer-Enhancing Techniques

Some techniques are validated to be effective in enhancing the transferability in classification. Among them, Diverse Input (DI) [9], Translation-Invariant (TI) [15] and [11] Scale-Invariant (SI) are three of the best ones. We are curious about whether they also work well in object detection.

In our experiment, DI [9] transforms 4 times with probability p ($p = 1$ for better transferability as suggested) and averaging the gradients. SI [11] divides the sample numerically by the power 2 for 4 times before gradient calculation. TI [15] adopts a kernel size of 15 as suggested.

From the results in Table 2, we discover that DI and TI do not have a significant increase of transferability in object detection. In comparison, SI is quite effective, further decreasing the mAP from the baseline. The mAP50 and mAP75 follow the same trend as in the Supplement Material.

Table 2: mAP of object detection by ATTACTION with transfer techniques on M2 (YOLOv3)

Method	M1	M2	M3	M4	M5	M6	M7	M8
ATTACTION	18.1	1.2	19.9	20.5	24.3	22.6	26.4	28.2
DI-ATTACTION	18.1	1.0	19.9	20.5	23.9	22.4	26.3	27.9
TI-ATTACTION	17.0	2.4	20.8	20.8	25.2	23.0	27.9	29.7
SI-ATTACTION	14.6	0.7	16.3	17.0	20.4	19.1	22.3	23.8

4.4 Transferability to Semantic Segmentation

Detection and segmentation are similar in some aspects, so they could be solved by one network [36, 45, 38]. Given the shared layers of two tasks, adversarial samples for object detection may transfer to semantic segmentation [17]. Accordingly, we evaluate this cross-task transferability by adversarial samples generated from SI-ATTACTION on surrogate model M2 (YOLOv3 [37]), M3 (RetinaNet [48]) and M5 (Mask R-CNN [36]).

From the results in Table 3, we find that SI-ATTACKION, the highest-transferable method, could also greatly hurt the performance of semantic segmentation, leading to a drop on mAP of over 70%. This might inspire the segmentation attackers to indirectly attack object detection.

Table 3: Segmentation mAP of SI-ATTACKION on M2 (YOLOv3)

Surrogate	mAP			mAP50			mAP75		
	M5	M7	M8	M5	M7	M8	M5	M7	M8
None	38.0	39.4	40.8	60.6	61.3	63.3	40.9	42.9	44.1
Ablation	31.0	31.9	33.5	51.2	51.0	53.7	32.4	34.3	35.4
M2	17.9	18.6	20.3	31.6	31.7	34.5	18.0	18.9	20.7
M3	11.6	11.9	12.9	19.2	19.1	20.7	12.1	12.6	13.7
M5	1.2	11.1	11.8	2.4	17.9	18.9	1.0	11.9	12.6

4.5 Visual Results

We present the visual results for ATTACKION to further illustrate its influence. For white-box scenarios in Fig. 4, the three models correctly detect a “person” and a “skateboard”, and the attention heat map is clear and structured. After ATTACKION, the heat maps are induced to be meaningless and without correct focus, leading to incorrect predictions, i.e., no or false detection.

For black-box scenarios in Fig. 5, we visualize several predictions on the same adversarial sample by black-box models. The objects in the image, e.g., laptop and keyboard, are quite large and obvious to detect. However, with a small perturbation from ATTACKION, 5 black-box models all fail to detect the laptop, keyboard and mouse. Surprisingly, 4 of them even detect a non-existent “bed”, which is neither relevant nor similar in the image.

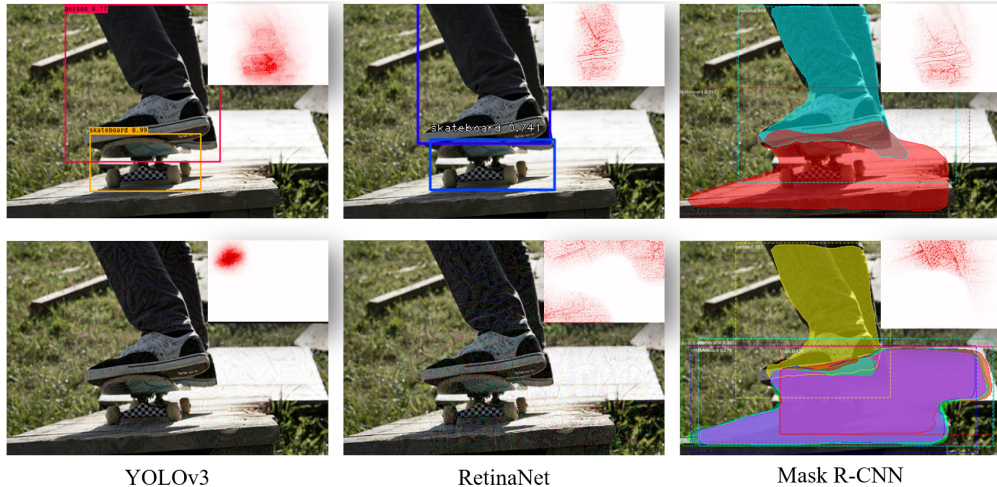


Figure 4: White-box attack illustration of ATTACKION. The image contains a person and a skateboard. The top row shows the original correct predictions and the corresponding heat maps for YOLOv3, RetinaNet and Mask R-CNN. The bottom row displays those for adversarial samples generated by attacking corresponding models. Note that there are several incorrect overlapped bounding boxes and masks (“car”, “motorcycle” and “boat”) in the image at the bottom right.

5 Adversarial Objects in Context

Given the great transferability of ATTACKION, we create Adversarial Objects in Context (AOCO), the first adversarial dataset for object detection. AOCO is generated from the full COCO 2017 validation set [23] with 5k samples. It contains 5K adversarial samples for evaluating object detection (AOCO detection) and 5K for semantic segmentation (AOCO segmentation). Samples in AOCO detection have the long side 416 and that for AOCO segmentation is 448.

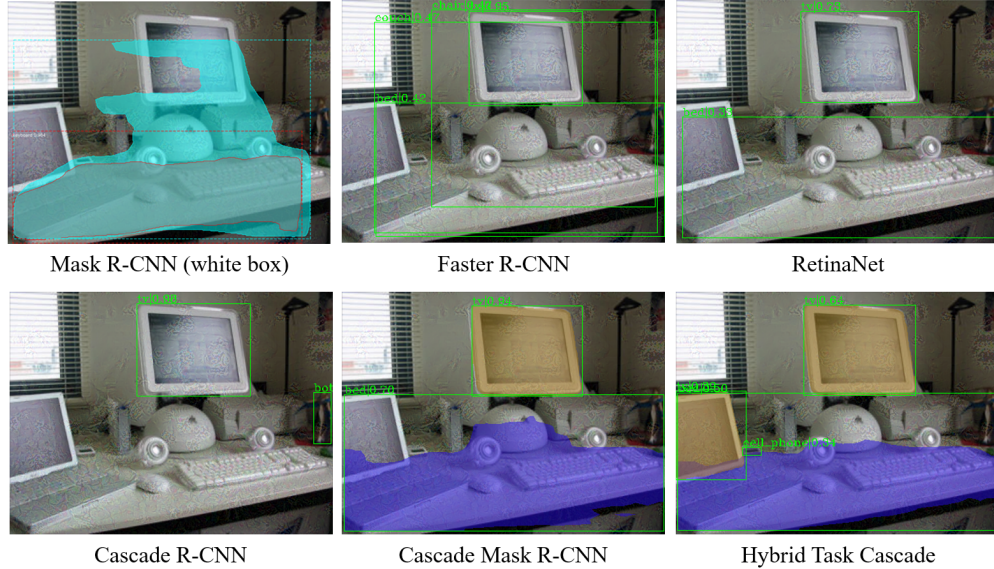


Figure 5: Black-box attack illustration of ATTENTION. Here are the predictions of the same adversarial sample generated by attacking Mask R-CNN. The sample contains “TV”, “laptop”, “mouse” and two “keyboard”s, but several black-box models only detect TV. They also produce incorrect bounding boxes or masks such as “bed”, “coach” and “chair”.

All 10K samples in AOCO are crafted by SI-ATTENTION, the highest-transferable method on object detection. The surrogate model we attack is YOLOv3 for AOCO detection and Mask R-CNN for AOCO segmentation given the results in Table 1 and Table 3.

We measure the degree of perturbation Δx in AOCO by Root Mean Squared Error (RMSE) as in [17, 50]. It is calculated as $\sqrt{\sum_i (\Delta x_i)^2 / N}$ in a pixel-wise way, and N is the size of the image. Performance of AOCO is reported in Table 4 (**bold** for white-box results). The RMSE in AOCO is lower than that in [51], and the perturbation is quite imperceptible. Adversarial samples in AOCO are demonstrated in the Supplement Material.

Table 4: Detection mAP and segmentation mAP on COCO and AOCO

	RMSE	M1	M2	M3	M4	M5	M6	M7	M8
COCO detection	0.000	29.3	33.4	38.1	40.7	42.1	42.5	45.7	46.9
AOCO detection	6.469	14.6	0.7	16.3	17	20.4	19.1	22.3	23.8
COCO segmentation	0.000	\	\	\	\	38.0	\	39.4	40.8
AOCO segmentation	6.606	\	\	\	\	1.2	\	11.1	11.8

6 Conclusion

To pursue a high attack transferability, this paper proposes ATTENTION, which suppresses the multi-node attention, a common property across calculated by our MN-SGLRP, to attack and therefore achieves a state-of-the-art transferability towards black-box models. We also empirically find that transfer techniques may help as well and the adversarial samples in detection transfer towards segmentation. Given the great transferability of ATTENTION, we generate Adversarial Objects in COntext (AOCO), the first adversarial dataset on object detection networks, which could help network designers to quickly evaluate and improve the robustness of detection networks.

Moreover, ATTENTION is worthy of further study. Other choices of multiple-node for attention might lead to a better performance, and it is valuable to test the transferability by attacking more surrogate models. Also, attention is just one common property and attacking on others is promising to have great transferability.

Broader Impact

Black-box adversarial samples for object detection pose a great threat to our real world because DNNs are implemented in scenarios from mobile devices to large-scale systems. ATTACTION would threat the security system is a calculated perturbation is added digitally in the camera. If we embed the ATTACTION perturbation inside the detection software, an autopilot car in high speed may be fooled by even one-frame adversarial patch [52] and crashed before manual control. If ATTACTION is conducted physically, the lawbreakers may wear a specific glass to unlock a random mobile phone or bypass the surveillance [13] and conduct an unauthorized entry.

Since the attacks proposed in this paper focus on transferable black-box attacks, they would exert greater damage compared to white-box attacks [2, 3, 4]. But our aim is not to beat DNNs maliciously, but to reveal their weakness, interpret them and help other researchers to improve their robustness. Accordingly, to mitigate the potential negative impacts of our work to the society, we release the AOCO dataset. They contain thousands of high-transferable adversarial samples in our experiment, and therefore could be used by DNN designers to test or improve the robustness of detection networks.

Acknowledgments and Disclosure of Funding

This work was partially supported by National Key Research Development Project (No. 2018AAA0100702), National Natural Science Foundation of China (No. 61977046), and 1000-Talent Plan (Young Program).

References

- [1] C. Szegedy, W. Zaremba, I. Sutskever, J. Bruna, D. Erhan, I. J. Goodfellow, and R. Fergus, “Intriguing properties of neural networks,” in *2nd International Conference on Learning Representations, ICLR 2014, Banff, AB, Canada, April 14-16, 2014, Conference Track Proceedings*, 2014.
- [2] I. J. Goodfellow, J. Shlens, and C. Szegedy, “Explaining and harnessing adversarial examples,” *STAT*, vol. 1050, p. 20, 2015.
- [3] N. Carlini and D. Wagner, “Towards evaluating the robustness of neural networks,” in *2017 IEEE Symposium on Security and Privacy (SP)*. IEEE, 2017, pp. 39–57.
- [4] A. Mądry, A. Makelov, L. Schmidt, D. Tsipras, and A. Vladu, “Towards deep learning models resistant to adversarial attacks,” *STAT*, vol. 1050, p. 9, 2017.
- [5] J. Su, D. V. Vargas, and K. Sakurai, “One pixel attack for fooling deep neural networks,” *IEEE Transactions on Evolutionary Computation*, 2019.
- [6] S. Baluja and I. Fischer, “Adversarial transformation networks: Learning to generate adversarial examples,” *arXiv preprint arXiv:1703.09387*, 2017.
- [7] N. Papernot, P. McDaniel, and I. Goodfellow, “Transferability in machine learning: from phenomena to black-box attacks using adversarial samples,” *arXiv preprint arXiv:1605.07277*, 2016.
- [8] W. Brendel, J. Rauber, and M. Bethge, “Decision-based adversarial attacks: Reliable attacks against black-box machine learning models,” in *6th International Conference on Learning Representations, ICLR 2018, Vancouver, BC, Canada, April 30 - May 3, 2018, Conference Track Proceedings*, 2018.
- [9] C. Xie, Z. Zhang, Y. Zhou, S. Bai, J. Wang, Z. Ren, and A. L. Yuille, “Improving transferability of adversarial examples with input diversity,” in *Proceedings of the IEEE Conference on Computer Vision and Pattern Recognition*, 2019, pp. 2730–2739.
- [10] Y. Dong, F. Liao, T. Pang, H. Su, J. Zhu, X. Hu, and J. Li, “Boosting adversarial attacks with momentum,” in *Proceedings of the IEEE Conference on Computer Vision and Pattern Recognition*, 2018, pp. 9185–9193.
- [11] *Nesterov Accelerated Gradient and Scale Invariance for Improving Transferability of Adversarial Examples*, 2020.
- [12] S. Chen, Z. He, C. Sun, and X. Huang, “Universal adversarial attack on attention and the resulting dataset damagenet,” *arXiv preprint arXiv:2001.06325*, 2020.
- [13] H. Zhang and J. Wang, “Towards adversarially robust object detection,” in *Proceedings of the IEEE International Conference on Computer Vision*, 2019, pp. 421–430.
- [14] S. Thys, W. Van Ranst, and T. Goedemé, “Fooling automated surveillance cameras: adversarial patches to attack person detection,” in *Proceedings of the IEEE Conference on Computer Vision and Pattern Recognition Workshops*, 2019.

- [15] Y. Dong, T. Pang, H. Su, and J. Zhu, “Evading defenses to transferable adversarial examples by translation-invariant attacks,” in *Proceedings of the IEEE Conference on Computer Vision and Pattern Recognition*, 2019, pp. 4312–4321.
- [16] T. Zhang and Z. Zhu, “Interpreting adversarially trained convolutional neural networks,” in *Proceedings of the 36th International Conference on Machine Learning, ICML 2019, 9-15 June 2019, Long Beach, California, USA*, 2019, pp. 7502–7511.
- [17] C. Xie, J. Wang, Z. Zhang, Y. Zhou, L. Xie, and A. Yuille, “Adversarial examples for semantic segmentation and object detection,” in *Proceedings of the IEEE International Conference on Computer Vision*, 2017, pp. 1369–1378.
- [18] Y. Li, D. Tian, X. Bian, S. Lyu, *et al.*, “Robust adversarial perturbation on deep proposal-based models,” 2018.
- [19] Y. Li, X. Bian, and S. Lyu, “Attacking object detectors via imperceptible patches on background,” *CoRR*, abs/1809.05966, 2018.
- [20] S. Bach, A. Binder, G. Montavon, F. Klauschen, K.-R. Müller, and W. Samek, “On pixel-wise explanations for non-linear classifier decisions by layer-wise relevance propagation,” *PloS one*, vol. 10, no. 7, 2015.
- [21] J. Gu, Y. Yang, and V. Tresp, “Understanding individual decisions of cnns via contrastive backpropagation,” in *Asian Conference on Computer Vision*. Springer, 2018, pp. 119–134.
- [22] B. K. Iwana, R. Kuroki, and S. Uchida, “Explaining convolutional neural networks using softmax gradient layer-wise relevance propagation.”
- [23] T.-Y. Lin, M. Maire, S. Belongie, J. Hays, P. Perona, D. Ramanan, P. Dollár, and C. L. Zitnick, “Microsoft coco: Common objects in context,” in *European Conference on Computer Vision*. Springer, 2014, pp. 740–755.
- [24] N. Papernot, P. McDaniel, I. Goodfellow, S. Jha, Z. B. Celik, and A. Swami, “Practical black-box attacks against machine learning,” in *Proceedings of the 2017 ACM on Asia Conference on Computer and Communications Security*. ACM, 2017, pp. 506–519.
- [25] J. Lu, H. Sibai, and E. Fabry, “Adversarial examples that fool detectors,” *arXiv preprint arXiv:1712.02494*, 2017.
- [26] Y. Li, X. Bian, M.-C. Chang, and S. Lyu, “Exploring the vulnerability of single shot module in object detectors via imperceptible background patches,” 2018.
- [27] Y. Wang, Y.-a. Tan, W. Zhang, Y. Zhao, and X. Kuang, “An adversarial attack on dnn-based black-box object detectors,” *Journal of Network and Computer Applications*, p. 102634, 2020.
- [28] R. R. Selvaraju, M. Cogswell, A. Das, R. Vedantam, D. Parikh, and D. Batra, “Grad-cam: Visual explanations from deep networks via gradient-based localization,” in *Proceedings of the IEEE International Conference on Computer Vision*, 2017, pp. 618–626.
- [29] M. D. Zeiler and R. Fergus, “Visualizing and understanding convolutional networks,” in *European Conference on Computer Vision*. Springer, 2014, pp. 818–833.
- [30] A. Shrikumar, P. Greenside, and A. Kundaje, “Learning important features through propagating activation differences,” in *Proceedings of the 34th International Conference on Machine Learning-Volume 70*. JMLR.org, 2017, pp. 3145–3153.
- [31] K. Simonyan and A. Zisserman, “Very deep convolutional networks for large-scale image recognition,” in *3rd International Conference on Learning Representations, San Diego, CA, USA, May 7-9, 2015, Conference Track Proceedings*, 2015.
- [32] K. He, X. Zhang, S. Ren, and J. Sun, “Deep residual learning for image recognition,” in *Proceedings of the IEEE Conference on Computer Vision and Pattern Recognition*, 2016, pp. 770–778.
- [33] G. Huang, Z. Liu, L. van der Maaten, and K. Q. Weinberger, “Densely connected convolutional networks,” in *2017 IEEE Conference on Computer Vision and Pattern Recognition, CVPR 2017, Honolulu, HI, USA, July 21-26, 2017*, 2017, pp. 2261–2269.
- [34] C. Szegedy, S. Ioffe, V. Vanhoucke, and A. A. Alemi, “Inception-v4, inception-resnet and the impact of residual connections on learning,” in *Proceedings of the Thirty-First AAAI Conference on Artificial Intelligence, February 4-9, 2017, San Francisco, California, USA*, 2017, pp. 4278–4284.
- [35] S. Ren, K. He, R. Girshick, and J. Sun, “Faster r-cnn: Towards real-time object detection with region proposal networks,” in *Advances in Neural Information Processing Systems*, 2015, pp. 91–99.
- [36] K. He, G. Gkioxari, P. Dollár, and R. Girshick, “Mask r-cnn,” in *Proceedings of the IEEE international conference on computer vision*, 2017, pp. 2961–2969.
- [37] J. Redmon and A. Farhadi, “Yolov3: An incremental improvement,” *arXiv preprint arXiv:1804.02767*, 2018.

- [38] K. Chen, J. Pang, J. Wang, Y. Xiong, X. Li, S. Sun, W. Feng, Z. Liu, J. Shi, W. Ouyang, *et al.*, “Hybrid task cascade for instance segmentation,” in *Proceedings of the IEEE Conference on Computer Vision and Pattern Recognition*, 2019, pp. 4974–4983.
- [39] F. Chollet *et al.*, “Keras,” <https://keras.io>, 2015.
- [40] M. Abadi, A. Agarwal, P. Barham, E. Brevdo, Z. Chen, C. Citro, G. S. Corrado, A. Davis, J. Dean, M. Devin, S. Ghemawat, I. Goodfellow, A. Harp, G. Irving, M. Isard, Y. Jia, R. Jozefowicz, L. Kaiser, M. Kudlur, J. Levenberg, D. Mané, R. Monga, S. Moore, D. Murray, C. Olah, M. Schuster, J. Shlens, B. Steiner, I. Sutskever, K. Talwar, P. Tucker, V. Vanhoucke, V. Vasudevan, F. Viégas, O. Vinyals, P. Warden, M. Wattenberg, M. Wicke, Y. Yu, and X. Zheng, “TensorFlow: Large-scale machine learning on heterogeneous systems,” 2015, software available from tensorflow.org. [Online]. Available: <https://www.tensorflow.org/>
- [41] A. Paszke, S. Gross, F. Massa, A. Lerer, J. Bradbury, G. Chanan, T. Killeen, Z. Lin, N. Gimelshein, L. Antiga, *et al.*, “Pytorch: An imperative style, high-performance deep learning library,” in *Advances in Neural Information Processing Systems*, 2019, pp. 8024–8035.
- [42] M. Alber, S. Lapuschkin, P. Seegerer, M. Hägele, K. T. Schütt, G. Montavon, W. Samek, K.-R. Müller, S. Dähne, and P.-J. Kindermans, “investigate neural networks,” *Journal of Machine Learning Research*, vol. 20, no. 93, pp. 1–8, 2019.
- [43] K. Chen, J. Wang, J. Pang, Y. Cao, Y. Xiong, X. Li, S. Sun, W. Feng, Z. Liu, J. Xu, *et al.*, “Mmdetection: Open mmlab detection toolbox and benchmark,” *arXiv preprint arXiv:1906.07155*, 2019.
- [44] W. Liu, D. Anguelov, D. Erhan, C. Szegedy, S. Reed, C.-Y. Fu, and A. C. Berg, “Ssd: Single shot multibox detector,” in *European Conference on Computer Vision*. Springer, 2016, pp. 21–37.
- [45] Z. Cai and N. Vasconcelos, “Cascade r-cnn: Delving into high quality object detection,” in *Proceedings of the IEEE Conference on Computer Vision and Pattern Recognition*, 2018, pp. 6154–6162.
- [46] qqwweee, “Yolov3 on keras and tensorflow,” <https://github.com/qqwweee/keras-yolo3>, 2018.
- [47] R. G. K. H. sung Yi Lin, Priya Goyal and P. Dollár, “Keras implementation of retinanet object detection,” <https://github.com/fizyr/keras-retinanet>, 2017.
- [48] T.-Y. Lin, P. Goyal, R. Girshick, K. He, and P. Dollár, “Focal loss for dense object detection,” in *Proceedings of the IEEE international conference on computer vision*, 2017, pp. 2980–2988.
- [49] W. Abdulla, “Mask r-cnn for object detection and instance segmentation on keras and tensorflow,” https://github.com/matterport/Mask_RCNN, 2017.
- [50] Y. Liu, X. Chen, C. Liu, and D. Song, “Delving into transferable adversarial examples and black-box attacks,” in *Proceedings of 5th International Conference on Learning Representations*, 2017.
- [51] D. Wu, Y. Wang, S. Xia, J. Bailey, and X. Ma, “Skip connections matter: On the transferability of adversarial examples generated with resnets,” in *Proceedings of the International Conference on Learning Representations*, 2019.
- [52] Y. Jia, Y. Lu, J. Shen, Q. A. Chen, H. Chen, Z. Zhong, and T. Wei, “Fooling detection alone is not enough: Adversarial attack against multiple object tracking,” in *International Conference on Learning Representations*, 2019.